Supplementary Figures

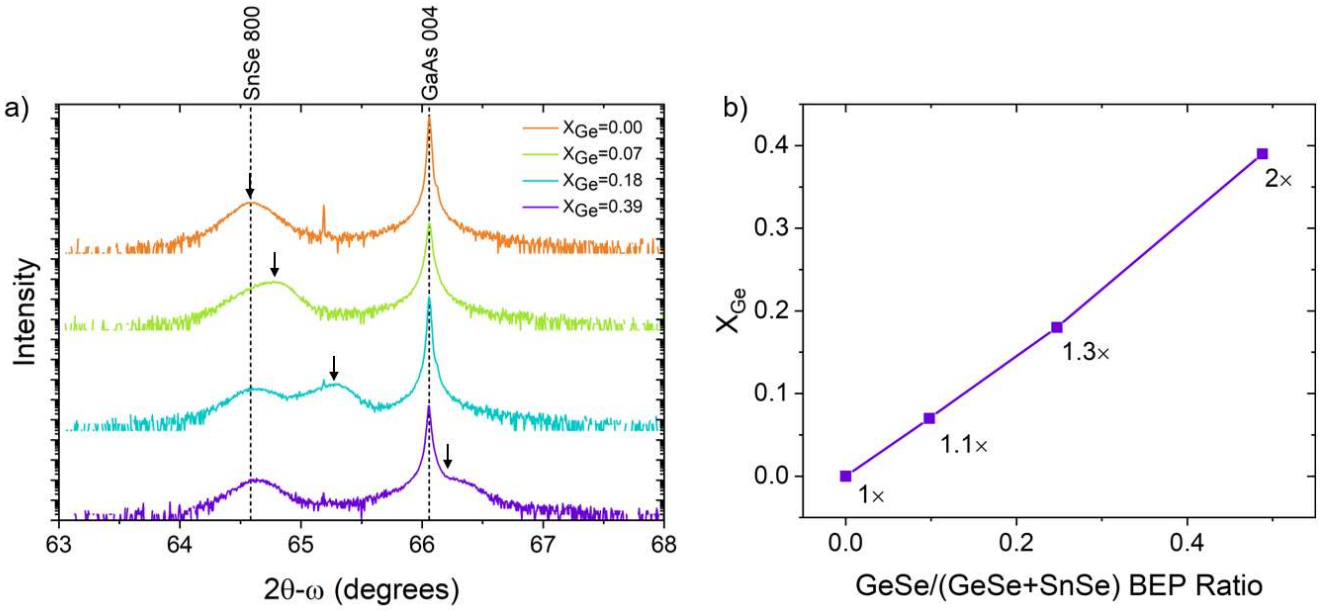

Figure S1. (a) Triple-axis symmetric 2θ-ω scans of various compositions of $Sn_{1-x}Ge_xSe$ alloys on GaAs(001). At X_{Ge}=0, the SnSe (800) reflection is from both the high temperature SnSe buffer and lower temperature SnSe film. When GeSe flux is added to SnSe, a SnGeSe peak emerges in addition to the SnSe buffer peak. As the Ge content increases, the SnGeSe peak shifts to higher 2θ-ω values implying the out of plane lattice parameter decreases due to the addition of Ge. (b) SnSe (800) peak positions are used to calculate Ge composition as a function of beam equivalent pressure (BEP) ratio. The growth rate was scaled by the multiplier next to each point as the total BEP was increased.

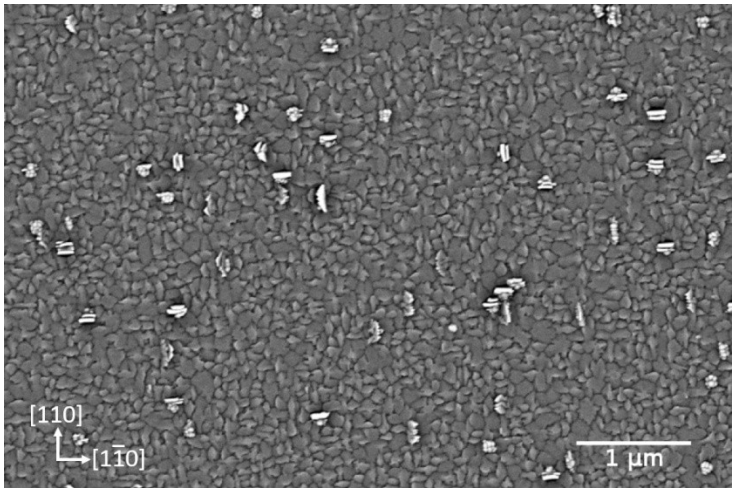

Figure S2. Plan-view scanning electron microscopy image of the $Sn_{0.61}Ge_{0.39}Se$ film grown on GaAs(001) shows $Sn_{0.61}Ge_{0.39}Se$ overgrowths and misorientations. Lattice directions of the GaAs substrate are labeled.

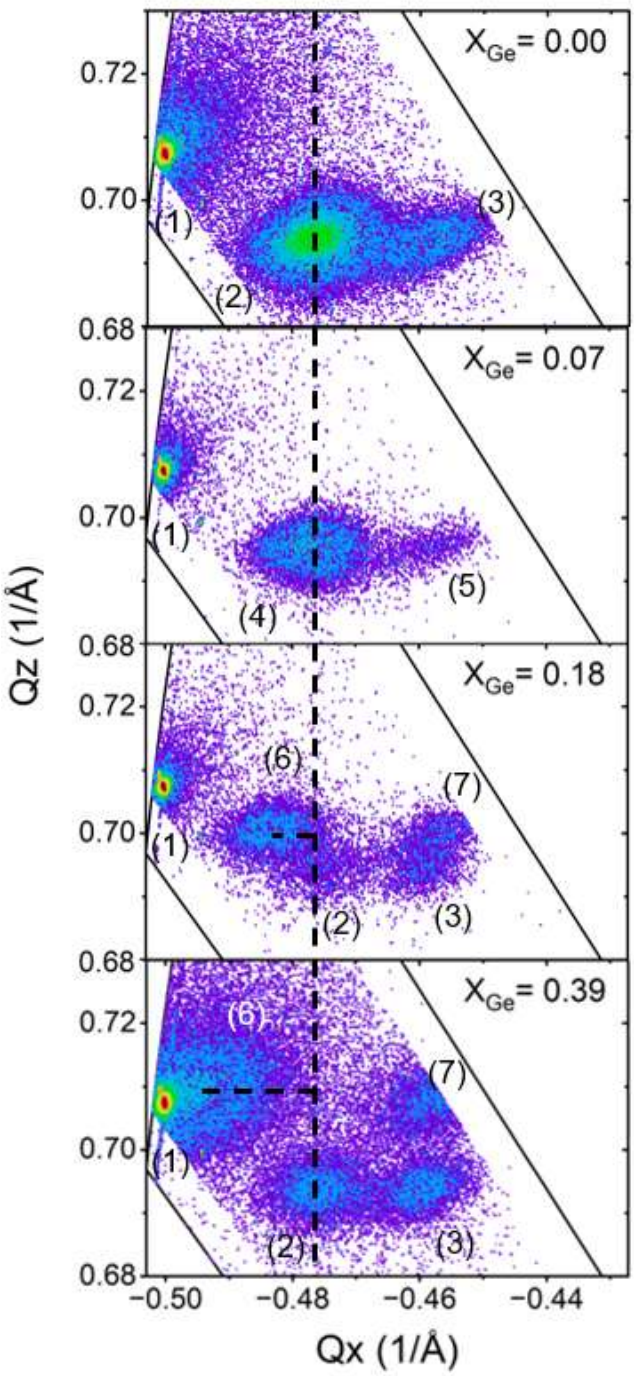

Figure S3. Reciprocal space maps of various compositions of SnGeSe alloys on GaAs(001). The 7 labels correspond to: (1) GaAs (224) peak, (2) SnSe (820) peak, (3) SnSe (802) peak, (4) a combination of the SnGeSe and SnSe buffer (820) peaks, (5) a combination of the SnGeSe and SnSe buffer (802) peaks, (6) SnGeSe (820) peak, and (7) SnGeSe (802) peak. The deviation of the GeSe (820) peak is marked by the dashed lines. The (820) and (802) alloy peaks shift as the in-plane lattice parameters 'b' and 'c' decrease with increased Ge content.